PCCP

Preparation of nanocrystalline ceria particles by sonochemical and microwave assisted heating methods

Hui Wang,[a] Jun-Jie Zhu,*[a] Jian-Min Zhu,[b] Xue-Hong Liao,[ac] Shu Xu,[a] Tao Ding[a] and Hong-Yuan Chen[a]

[a] *Laboratory of Mesoscopic Materials Science and State Key Laboratory of Coordination Chemistry, Department of Chemistry, Nanjing University, Nanjing 210093, People's Republic of China. E-mail: jjzhu@nju.edu.cn*

[b] *National Laboratory of Solid State of Microstructures, Nanjing University, Nanjing 210093, People's Republic of China*

[c] *Huanggang Normal University, Huangzhou 438000, Hubei, People's Republic of China*

Received 7th February 2002, Accepted 23rd May 2002
First published as an Advance Article on the web 19th June 2002

Nanocrystalline ceria (CeO_2) particles have been successfully prepared *via* sonochemical and microwave assisted heating routes from aqueous solutions containing $(NH_4)_2Ce(NO_3)_6$, hexamethylenetetramine and poly (ethylene glycol)-19000 (PEG). The products were characterized by techniques such as powder X-ray diffraction, transmission electron microscopy, high-resolution transmission electron microscopy, selected area electron diffraction, Brunauer–Emmett–Teller nitrogen adsorption and UV–Visible absorption spectroscopy. Analysis of the results showed that the products had uniform shape, narrow size distribution and displayed conspicuous quantum size effects.

Introduction

Ceria (CeO_2) is a rare earth oxide that has been attracting great interest due to its unique properties and wide applications. It is a highly refractory oxide and has the fluorite structure which is stable from room temperature to its melting point. It is also of considerable interest due to its close parameter matching with silicon (0.35% lattice mismatch) and strong ultraviolet absorption. It can be used as an additive to glass (2–4%) to protect light-sensitive materials, as a coating for corrosion protection of metals, as an oxidation catalyst, and as a counter electrode for electrochromic devices.[1] It is currently also used as an oxygen ion conductor in solid oxide fuel cell, electrolyzers, oxygen pumps and amperometric oxygen monitors owing to its high oxygen ion conductivity.[2] It also has potential applicability to silicon-on-insulator structure, stable capacitor devices for large-scale integration, and stable buffer layers between high temperature superconducting materials and silicon substrate.[3]

Many studies on the preparation of CeO_2 fine powders have been conducted using techniques such as hydrothermal synthesis,[2,4] a reversed micelles route,[5] coprecipitation,[6,7] forced hydrolysis,[8] an electrochemical method,[9] decomposition of oxalate precursors,[10] urea-based or hexamethylenetetramine-based homogeneous precipitation,[11–14] the use of hydrazine monohydrate,[15] solvothermal synthesis,[16] and solid-state reactions at room temperature.[17,18] It is also reported that a transparent colloidal solution of ultrafine CeO_2 particles can be obtained by the reaction of cerium metal in 2-methoxyethanol at 200–300 °C.[19] Various techniques have also been developed for the preparation of nanometre CeO_2 thin films including metal–organic chemical vapour deposition (MOCVD), electrodeposition and spray pyrolysis.[20–23]

In recent years, ultrasound and microwave irradiation have been extensively used to generate novel materials with unusual properties. Ultrasound irradiation can induce the formation of particles with a much smaller size and higher surface area than those reported by other methods.[24] The effects arise from acoustic cavitation, that is, the formation, growth and implosive collapse of bubbles in a liquid. The implosive collapse of the bubbles generates a localized hotspot though adiabatic compression or shock wave formation within the gas phase of the collapsing bubbles. The conditions in these hotspots have been experimentally determined, finding a transient temperature of ~5000 K, pressure of >1800 atm and cooling rates in excess of 10^{10} K s^{-1}.[25a] These extreme conditions during ultrasound irradiation have been successfully applied to prepare various nanosized materials including metals,[25a,26] metal carbides,[27] metal oxides[28] and metal chalcogenides.[29] Microwave irradiation as a heating method, which is generally quite fast, simple and efficient in energy, has been developed and is widely used in various fields in chemistry.[30] It is known that the interaction of dielectric materials, liquids or solids, with microwaves leads to what is generally known as dielectric heating. Electric dipoles present in such materials respond to the applied electric field. In liquids, this constant reorientation leads to friction between molecules, which subsequently generates heat. Claimed effects of microwave irradiation include thermal and non-thermal effects.[30] The application of microwave irradiation in the preparation of nanoparticles has been reported in recent years.[31–35] The application of microwave irradiation to materials science has shown very rapid growth due to its unique reaction effects such as rapid volumetric heating and the consequent dramatic increase in reaction rates, *etc*.

Recently, ceria nanoparticles have been prepared sonochemically, using cerium nitrate and azodicarbonamide as the starting materials, and ethylenediamine or tetraalkylammonium hydroxide as the additives.[36] In a recent communication, we applied microwave techniques to the synthesis of nanocrystalline CeO_2 powders.[37] In this paper, we give a detailed description of the preparation of nanocrystalline ceria

 DOI: 10.1039/b201394k

particles based on the ultrasound-induced and microwave-induced hydrolysis of $(NH_4)_2Ce(NO_3)_6$in the presence of hexamethylenetetramine, using PEG as the dispersion stabilizer. The as-prepared ceria nanoparticles have uniform spherical morphology, narrow size distribution, and display conspicuous quantum size effects. It is found to be a convenient, mild, energy efficient route to produce the CeO_2 nanoparticles in only one step.

Experimental

All the reagents were of analytical purity. $(NH_4)_2Ce(NO_3)_6$, poly (ethylene glycol)-19000 (PEG) and hexamethylenetetramine were all purchased from Shanghai Chemistry Reagent Factory (China). Ultrasound irradiation was accomplished with a high-intensity ultrasound probe (Xinzhi Co., China; JY92-2D; 0.6 cm diameter; Ti-horn, 20 kHz, 60 W cm^{-2}) immersed directly in the reaction solution. Microwave-assisted reactions were conducted by using a microwave oven with 650 W power (Sanle general electric corp. Nanjing, China). A refluxing system was connected to the microwave oven.

In a typical procedure for the ultrasound-induced preparation, appropriate amounts of $(NH_4)_2Ce(NO_3)_6$, hexamethylenetetramine and poly(ethylene glycol)-19000 (PEG) were introduced into 100 mL distilled water to give final concentrations of 0.02 mol L^{-1} $(NH_4)_2Ce(NO_3)_6$, 0.1 mol L^{-1} hexamethylenetetramine and 0.5 wt.% PEG. Then the mixture was exposed to high-intensity ultrasound irradiation under ambient air for 30 min. The sonication was conducted without cooling so that a temperature of 343 K was reached at the end of the reaction.

To prepare ceria nanoparticles *via* the microwave-induced route, appropriate amount of $(NH_4)_2Ce(NO_3)_6$, hexamethylenetetramine and poly(ethylene glycol)-19000 (PEG) were introduced into 100 mL distilled water to give final concentrations of 0.02 mol L^{-1} $(NH_4)_2Ce(NO_3)_6$, 0.1 mol L^{-1} hexamethylenetetramine and 0.5 wt.% PEG. Then the mixture was placed in the microwave reflux system and refluxed under ambient air for 10 min. The microwave oven followed a working cycle of 9 s on and 21 s off (30% power).

The post-reaction treatment procedure is the same for both methods. After cooling to room temperature, the precipitates were centrifuged, washed with distilled water and acetone repeatedly, and dried in air. The final products were collected for characterization. The products were characterized by powder X-ray diffraction (XRD), transmission electron microscopy (TEM), selected area electron diffraction (SAED), high-resolution transmission electron microscopy (HRTEM), Brunauer–Emmett–Teller (BET) surface area measurements and UV–Visible absorption spectroscopy.

The XRD analysis was performed with a Shimadzu XD-3A X-ray diffractometer at a scanning rate of 4° min^{-1} in the 2θ range from 20° to 60°, with graphite monochromatized Cu-Kα radiation ($\lambda = 0.15418$ nm). TEM and SAED images were obtained with a JEOL JEM-200CX transmission electron microscope, using an accelerating voltage of 200 kV. The samples used for TEM observation were prepared by dispersing some products in ethanol followed by ultrasonic vibration for 30 min, then placing a drop of the dispersion onto a copper grid coated with a layer of amorphous carbon. The HRTEM images were obtained with a JEOL-4000EX high-resolution transmission electron microscope with a 400 kV accelerating voltage. The surface area (BET) measurements were carried out using a Micromeritics-Gemini surface area analyzer, employing nitrogen gas adsorption. A Ruili 1200 photospectrometer (Peking Analytical Instrument Co.) was used to record the UV–Visible absorption spectra of the as-prepared particles.

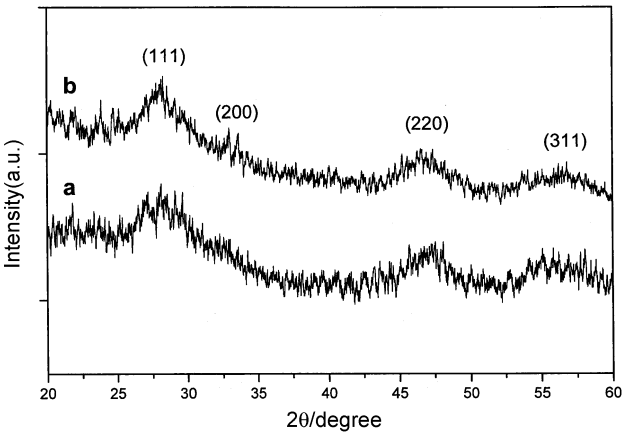

Fig. 1 Powder XRD patterns of CeO_2 nanoparticles (a) prepared by microwave irradiation; (b) prepared by ultrasonic irradiation.

Results and discussions

The powder XRD patterns of as-prepared Ceria nanoparticles are shown in Fig. 1. The sonochemical and microwave method yield the same solid phase for CeO_2. The diffraction peaks correspond to the (111), (200), (220) and (311) planes, which can be indexed to the pure cubic fluorite structure for CeO_2. No peak of any other phase is detected. The intensities and positions of the peaks are in perfect agreement with the literature values.[38] The broadening of the peaks indicates that the crystallite sizes are small. The average particle sizes of the products prepared by sonochemical and microwave-assisted method are calculated to be *ca.* 2.8 and *ca.* 2.6 nm respectively, according to the Debye–Scherrer equation.[39]

Fig. 2 shows the XRD patterns of the sonochemical product sintered at 300 °C, 500 °C and 700 °C for 2 h respectively. When the particles were sintered, no phases other than the cubic phase for CeO_2 were detected in the XRD patterns, but the XRD peaks became gradually sharper with increasing sintering temperature, indicating the increase in crystal size due to the sintering process that the particles undergo. The average sizes of the CeO_2 nanoparticles sintered at 300 °C, 500 °C and 700 °C are estimated to be *ca.* 5 nm, *ca.* 10 nm and *ca.* 20 nm respectively according to the Debye–Scherrer equation.

The size and morphology of the products are analyzed by the TEM images (Fig. 3). Fig. 3(a) reveals that the product prepared by the microwave method consists of well-dispersed

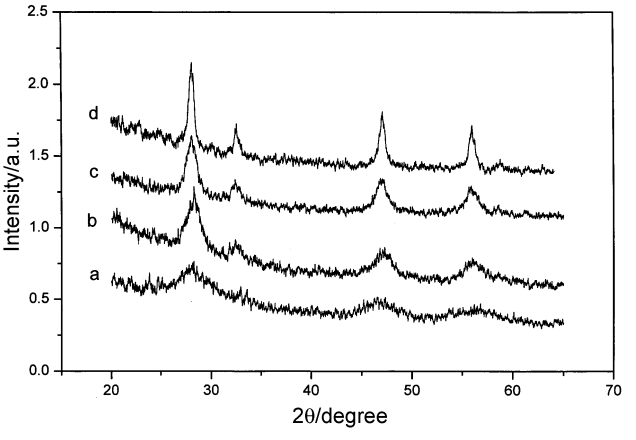

Fig. 2 Powder XRD patterns of CeO_2 nanoparticles prepared sonochemically sintered at different temperatures: (a) as-prepared; (b) sintered at 300 °C for 2 h; (c) sintered at 500 °C for 2 h; (d) sintered at 700 °C for 2 h.

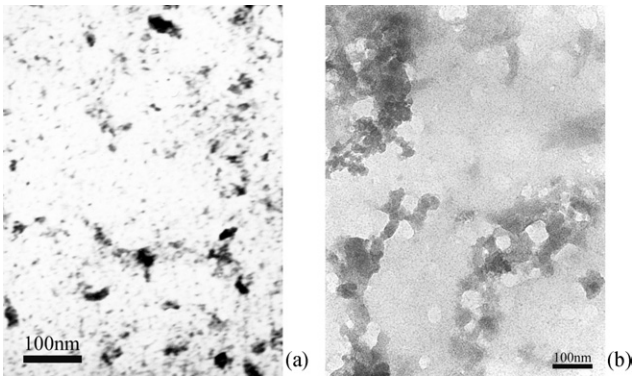

Fig. 3 TEM images of CeO_2 nanoparticles (a) prepared by microwave irradiation; (b) prepared by ultrasonic irradiation.

spherical nanoparticles whose diameter is in the range 2 to 3 nm,which is essentially identical with the result calculated from the XRD pattern. The particles prepared sonochemically are agglomerated, as observed in the TEM image (Fig. 3(b)), making it difficult to discriminate individual particles. The crystallinity and crystallography of the product are proven by selected area electron diffraction (SAED). Transmission electron diffraction performed on a set of such nanoparticles led to patterns as shown in Fig. 4. The SAED measurements show that the particles are crystallized and the diffraction rings match the XRD peaks very well.

The HRTEM images recorded on the as-prepared CeO_2 nanoparticles provide further insight into their structures. The HRTEM images of the products (Fig. 5) exhibit good crystallinity and clear lattice fringes. It is apparent that both products have regular spherical shapes and narrow size distributions. The product prepared sonochemically consists of 2–3 nm nanoparticles which are agglomerated together to form porous irregular networks, while the microwave-prepared product consists of monodisperse CeO_2 nanoparticles, as observed in the HRTEM images. The particle size distributions, measured directly from the HRTEM images, are shown as histograms in Fig. 6.

The surface area (BET) measurements were carried out by means of nitrogen gas adsorption. The BET surface area of the particles prepared sonochemically is measured to be 227.2191 ± 1.4053 m^2 g^{-1} and that of the microwave-prepared product is 251.0412 ± 1.8181 m^2 g^{-1}.

We have measured the UV–Visible absorption spectra of the product in order to resolve the excitonic or interband transitions of ceria nanoparticles. The UV–Visible absorption spectra of the products dispersed in ethanol are shown in Fig. 7. An

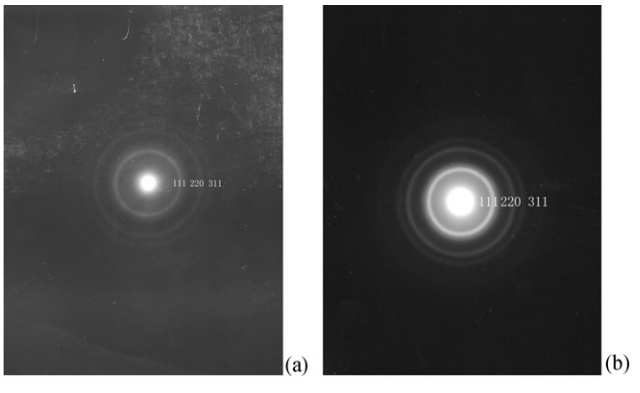

Fig. 4 SAED images of CeO_2 nanoparticles (a) prepared by microwave irradiation; (b) prepared by ultrasonic irradiation.

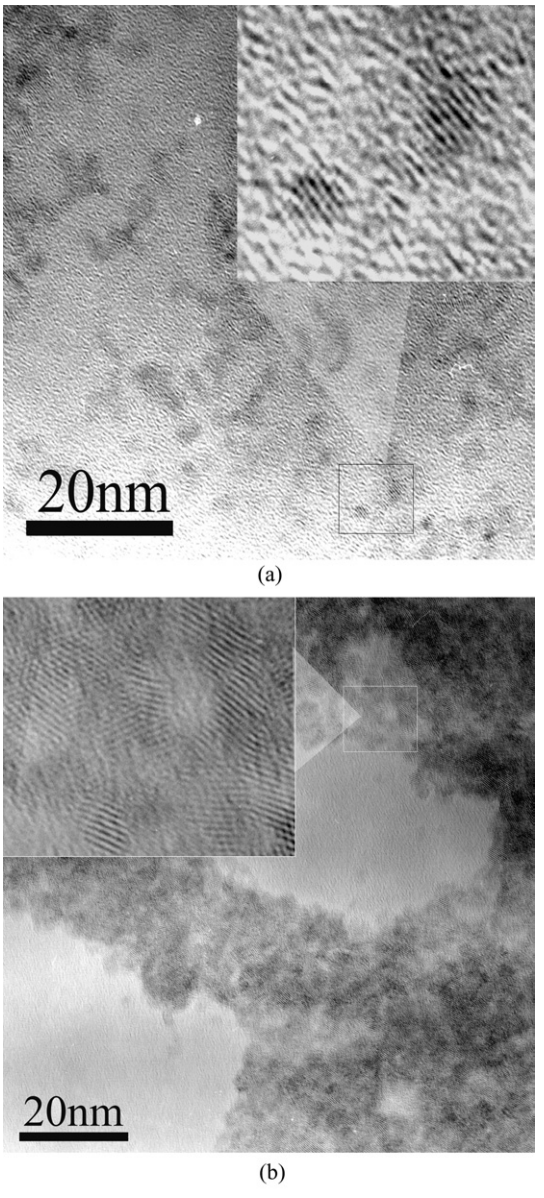

Fig. 5 HRTEM images of CeO_2 nanoparticles (a) prepared by microwave irradiation; (b) prepared by ultrasonic irradiation.

estimate of the optical band-gap is obtained using the following equation for a semiconductor:

$$\alpha(\nu) = A(h\nu/2 - E_g)^{m/2}$$

where A is a constant, α is the absorption coefficient and m equals 1 for a direct transition. The energy intercept of a plot of $(\alpha E_{phot})^2$ *versus* E_{phot} yields E_g for a direct transition (Fig. 8).[40] The band-gaps of the as-prepared CeO_2 nanoparticles are calculated to be 4.11 eV and 5.48 eV respectively from the UV–Visible absorption spectra, which is much larger than the reported value for bulk CeO_2 ($E_g = 3.19$ eV).[1] Light absorption leads to an electron in the conduction band and a positive hole in the valence band. In small particles they are confined to potential wells of small lateral dimension and the energy difference between the position of the conduction band and a free electron, which leads to a quantization of their energy levels. The phenomenon arises when the size of the particles becomes comparable to the de Broglie wavelength of a charge carrier. The increase in the band-gap of the as-prepared CeO_2 nanoparticles is indicative of size quantum effects.[41] Masui *et al.* reported the band-gaps of 4.1 nm and 2.6 nm CeO_2 nanoparticles prepared with reversed micelles to be

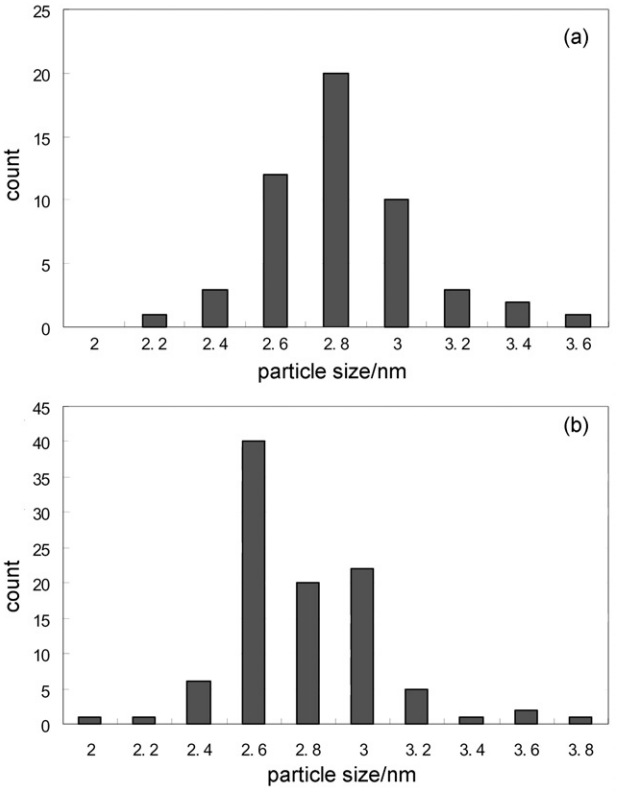

Fig. 6 The particle size distribution picture measured directly from HRTEM: (a) CeO_2 nanoparticles prepared by microwave heating method; (b) CeO_2 nanoparticles prepared by sonochemical method.

3.38 and 3.44 eV respectively.[5] Orel and Orel reported the quantum effects of thin films with band gap of 3.5–3.6 eV.[1] Gedanken and co-workers also reported the band gap of 3.3 nm CeO_2 nanoparticles prepared by the sonochemical method to be 3.68 eV.[36] Herein, the as-prepared CeO_2 nanoparticles are smaller than those reported, so the band-gaps become even larger.

It is noteworthy that the sonochemically prepared CeO_2 nanoparticles have a much larger band-gap than that of the product prepared by the microwave heating method though both products have similar average size and size distribution. In the case of the sonochemical preparation, a liquid–solid heterogeneous system is formed after nucleation of the CeO_2 nuclei. In such a system, the presence of ultrasound can

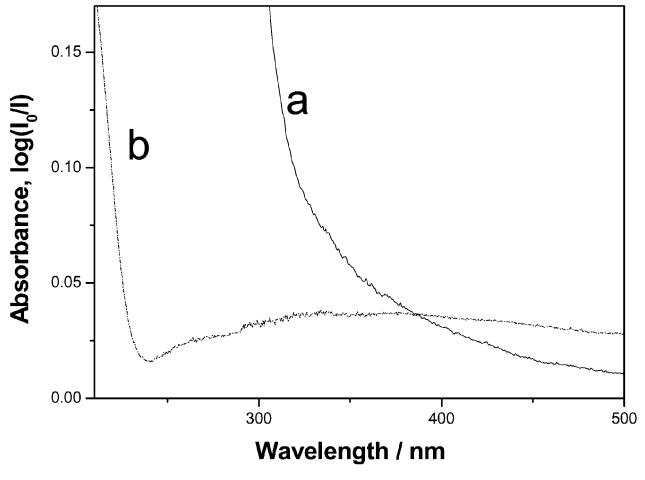

Fig. 7 The UV–Vis absorbance spectra of CeO_2 nanoparticles (a) prepared by microwave irradiation; (b) prepared by ultrasonic irradiation (in ethanol suspension).

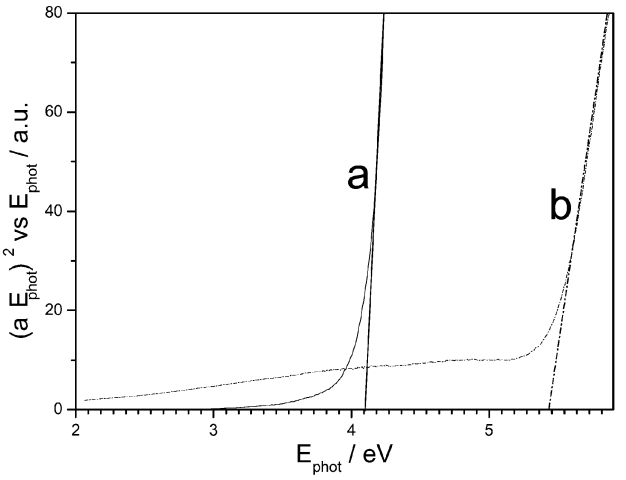

Fig. 8 Plots of $(\alpha E_{phot})^2$ *vs.* E_{phot} for direct transitions of CeO_2 nanoparticles (a) prepared by microwave irradiation; (b) prepared by ultrasonic irradiation.

enhance the reactions. The effects of interparticle collisions, microjets and shockwaves can drive high-speed jets of liquid to impinge upon the surface where they create a localized erosion to produce a newly exposed and highly active surface. Meanwhile, the ultrasound improves mass transport, and causes particle fragmentation which substantially increases the surface activity of the solid products which have a large number of dangling bonds, defects or traps on their surface. The increase in the band-gap of the product prepared sonochemically may be ascribed to the special surface state of this sample.

Hydrolysis refers to those reactions of metallic ions with water that liberate protons and produce hydroxide or oxide solids.[42] Ce^{4+} ions, which have a low basicity and high charge, undergo strong hydration. Firstly, Ce^{4+} ions are hydrolyzed and form complexes with water molecules or OH^- to give $[Ce(OH)_x(H_2O)_y]^{(4-x)+}$, where $x+y$ is the coordination number of Ce^{4+}. Further polymerization is likely, and both species can serve as the precursors for the final ceria nanoparticles. In an aqueous solution, H_2O, being a polar molecule, tends to take protons away from coordinated hydroxide, leading to the formation of $CeO_2{\cdot}nH_2O$. This process can be described by the following equations:

$$Ce^{4+} + xOH^- + yH_2O \rightarrow [Ce(OH)_x(H_2O)_y]^{(4-x)+}$$

$$[Ce(OH)_x(H_2O)_y]^{(4-x)+} + H_2O \rightarrow CeO_2 \cdot nH_2O + H_3O^+$$

It is well known that the hydroxylation of metal ions and the deprotonation can be greatly accelerated by raising the solution temperature or the pressure. When solutions are exposed to strong ultrasound, bubbles in the solution are implosively collapsed by acoustic fields, and high-temperature and high-pressure fields are produced at the centers of the bubbles. The CeO_2 nanoparticles are formed through the sonohydrolysis mechanism. Similar ideas have been described by Gedanken and co-workers[28b] when they tried to prepare CuO and ZnO nanoparticles sonochemically. The extreme conditions formed in the process of ultrasound irradiation can promote the hydrolysis of Ce^{4+} and are favorable for the formation of CeO_2 nanoparticles with highly uniform morphology, narrow size distribution and high purity. It is known that during the sonochemical process, three different regions[43] are formed: (a) the inner environment (gas phase) of the collapsing bubbles, where the elevated temperatures and pressures are produced, leading to the formation of $H^{\bullet}$ and $OH^{\bullet}$ radicals; (b) the interfacial region between the cavitation bubbles and the bulk solution where the temperature is lower than in the

gas-phase region but still high enough to induce a sonochemical reaction; (c) the bulk solution, which is at ambient temperature. Among the three regions mentioned above, it appears that the current sonochemical reaction occurs within the interfacial region, yielding nanoparticles, because of the very high quenching rate experienced by the products. If the reactions take place inside the collapsing bubbles, then the temperature inside the bubbles depends on the vapour pressure of the solvents. If water is used as the solvent, the maximum bubble core temperature that can be attained is approximately 4000 K.[25b] The product is amorphous as a result of the cooling rates ($>10^{10}$ K s^{-1}) which occur during the collapse.[25a] On the other hand, if the reactions take place within the interfacial region where the temperature has been measured to be 1900 K,[25c] one would expect to obtain nanocrystalline products. In the present study, water is used as the solvent and the product is nanocrystalline, which is proved by the results of XRD, SAED and HRTEM measurements. Therefore, we propose that the formation of CeO_2 occurs within the interfacial region.

In the case of microwave-induced hydrolysis, the reactions are driven by the intense collision and friction of the molecules. Microwaves are electromagnetic waves, which contain electric and magnetic field components. The force derived from these changes direction rapidly, which causes heat because the assembly of molecules cannot respond to it instantaneously, creating friction which manifests itself as heat. When incident microwaves are perpendicular to the surface of a material, their intensity decreases progressively inside the sample in the direction of incidence as the microwave energy is progressively dissipated, but for most materials, D (the distance in the direction of penetration at which the incident power is reduced to half its initial value) is quite large, and therefore, the power dissipation is fairly uniform throughout the materials. The formation of uniform nanosized particles demands a uniform growth environment, and microwave heating affords this. With microwave irradiation of reactants in polar solvents, temperature and concentration gradients can be avoided, providing a uniform environment for the nucleation.[35] Compared with conventional heating methods, microwave heating presents a more rapid and simultaneous nucleation due to the fast and homogeneous heating effects of microwaves.

It was found that the sonication time has little influence on the particle size and morphology. We found that after sonication for about 15 min, the stock solution turned yellowy turbid, indicating the formation of CeO_2 nuclei. After sonication for about 30 min, the reaction was complete. The CeO_2 nanoparticles obtained were stable, and their size and morphology did not present conspicuous change with the increase in sonication time. We have also carried out experiments to investigate the effects of the ultrasonic intensity. We find that it takes a longer period of time for the CeO_2 nuclei to form if the stock solution is exposed to ultrasound irradiation of a lower intensity. When we used a sonic intensity of 20 W cm^{-2} and all the other preparation conditions were kept unchanged, it was observed that the CeO_2 nuclei began to form after 25 min, and the as-prepared CeO_2nanoparticles were poorly crystalline, as observed from the XRD pattern and HRTEM image.

The influence of microwave power and reaction time on the formation of CeO_2 nanoparticles was investigated. When the microwave power is in the range 10% to 40%, the as-prepared CeO_2 nanoparticles are of similar size and morphology. Violent 'bump' boiling of the solvent occurs when the power is greater than 50%. When the reaction time was less than 5 min, no turbidity was observed and the solution remained transparent. After exposure to microwave irradiation for 8 min, it turned yellowy turbid, indicating the formation of the product. After 10 min, the reaction was complete, and the yield was as high as 90%. If the reaction time was prolonged to 30 min or even longer, the yield did not increase any more, and the size and morphology of the CeO_2 nanoparticles remained almost unchanged.

Conclusion

Sonochemical and microwave-assisted heating methods have been successfully established for the preparation of nanocrystalline CeO_2 particles. Both methods are found to be convenient, mild, efficient and environmentally friendly. It is predicted that scale-up of these methods may lead to large quantities of nanosized CeO_2 particles with wide applications. The methods can also be extended to the preparation of some other rare earth oxides nanocrystals.

Acknowledgements

This work is supported by the National Natural Science Foundation of China (No.50072006), the Jiangsu Science and Technology Foundation (BG 2001039) and Youth Foundation of Ministry of Education in Hubei Province, China (2001B43001). The authors also thank Ms Xiaoning Zhao from the Modern Analytic Center of Nanjing University for the TEM measurements. We are also grateful to Mr Jinzhong Xu for his kind assistance.

References

1 Z. C. Orel and B. Orel, *Phys. Status Solidi B*, 1994, **186**, K33.
2 M. Hirano and E. Kato, *J. Am. Ceram. Soc.*, 1996, **79**, 777.
3 L. Luo, X. D. Wu, R. C. Dye, R. E. Muenchausen, S. R. Folton, Y. Coulter, C. J. Maggiore and T. Inoue, *Appl. Phys. Lett.*, 1991, **59**, 2043.
4 (*a*) Y. C. Zhou and M. N. Rahaman, *J. Mater. Res.*, 1993, **8**, 1680; (*b*) M. Hirano and E. Kato, *J. Mater. Chem.*, 2000, **10**, 473.
5 T. Masui, K. Fujiwara, K. Machida, G. Adachi, T. Sakata and H. Mori, *Chem. Mater.*, 1997, **9**, 2197.
6 H. Yahiro, Y. Baba, K. Eguchi and H. Arai, *J. Electrochem. Soc.*, 1988, **135**, 2077.
7 T. J. Kirk and J. Winnick, *J. Electrochem. Soc.*, 1993, **140**, 3494.
8 W. P. Hsu, L. Ronnquist and E. Matijevic, *Langmuir*, 1988, **4**, 31.
9 Y. Zhow, R. J. Philips and J. A. Switzer, *J. Am. Ceram. Soc.*, 1995, **78**, 981.
10 J. V. Herie, T. Horita, T. Kawada, N. Sakai, H. Yokokawa and M. Dokiya, *J. Am. Ceram. Soc.*, 1997, **80**, 933.
11 E. Matijevic and W. P. Hsu, *J. Colloid Interface Sci.*, 1987, **118**, 506.
12 B. Aiken, W. P. Hsu and E. Matijevic, *J. Am. Ceram. Soc.*, 1988, **71**, 845.
13 P. L. Chen and I. W. Chen, *J. Am. Ceram. Soc.*, 1993, **76**, 1577.
14 P. L. Chen and I. W. Chen, *J. Am. Ceram. Soc.*, 1996, **79**, 3129.
15 S. Nakane, T. Tachi, M. Yoshinaka, K. Hirota and O. Yamaguchi, *J. Am. Ceram. Soc.*, 1997, **80**, 3221.
16 E. Verdon, M. Devalette and G. Damazeau, *Mater. Lett.*, 1995, **25**, 127.
17 F. Li, X. H. Yu, H. J. Pan, M. L. Wang and X. Q. Xin, *Solid State Sci.*, 2000, **2**, 767.
18 X. H. Yu, F. Li, X. R. Ye, X. Q. Xin and Z. L. Xue, *J. Am. Ceram. Soc.*, 2000, **83**, 964.
19 I. Masashi, K. Minoru and I. Tomoyuki, *Chem. Commun.*, 1999, 957.
20 F. Weiss, J. P. Senateur, C. Dubourdieu, V. Galindo and J. Lindner, *Vide-Science Technique ET Applications*, 1998, **53**, 561.
21 K. Konstantinov, I. Stambolova, P. Peshev, B. Dariet and S. Vassilev, *Int. J. Inorg. Mater.*, 2000, **2**, 277.
22 A. Mukherjee, D. Harrison and E. J. Podlaha, *Electrochem. Solid State Lett.*, 2001, **4**(9)D5.
23 M. VakketRegi, F. Conde, S. Nicolopoulos, C. V. Ragel and J. M. GonzakesCalbet, *Synth. Prop. Mech. Alloy Nanocryst. Mater.*, 1997, **235**, 291.
24 K. S. Suslick, *Ultrasound: Its Chemical, Physical and Biological Effects*, VCH, Weinheim, Germany, 1988.
25 (*a*) K. S. Suslick, S. B. Choe, A. A. Cichowlas and M. W. Grinstaff, *Nature*, 1991, **353**, 414; (*b*) V. Misik, N. Miyoshi and P. Riesz, *J. Phys. Chem.*, 1995, **99**, 3605; (*c*) W. B. McNamara, Y. T. Didenko and K. S. Suslick, *Nature*, 1999, **401**, 772.

26 (*a*) N. Aul Dhas, P. Paul Raj and A. Gedanken, *Chem. Mater.*, 1998, **10**, 1446; (*b*) N. Aul Dhas, H. Cohen and A. Gedanken, *J. Phys. Chem.*, 1997, **101**, 6834; (*c*) T. Fujimoto, S. Terauchi, H. Umehara, I. Kojima and W. Henderson, *Chem. Mater.*, 2001, **13**, 1057.

27 T. Hyeon, M. Fang and K. S. Suslick, *J. Am. Chem. Soc.*, 1996, **118**, 5492.

28 (*a*) N. Arul Dhas and A. Gedanken, *J. Phys. Chem. B*, 1997, **101**, 9495; (*b*) R. V. Kumar, Y. Diamant and A. Gedanken, *Chem. Mater.*, 2000, **12**, 2301; (*c*) X. Cao, Y. Koltypin, G. Katabi, I. Felner and A. Gedanken, *J. Mater. Res.*, 1997, **12**, 405; (*d*) J. J. Zhu, Z. H. Lu, S. T. Aruna, D. Aurbach and A. Gedanken, *Chem. Mater.*, 2000, **12**, 2557.

29 (*a*) J. J. Zhu, Y. Koltypin and A. Gedanken, *Chem. Mater.*, 2000, **12**, 73; (*b*) B. Li, Y. Xie, J. X. Huang, Y. Liu and Y. T. Qian, *Chem. Mater.*, 2000, **12**, 2641; (*c*) M. M. Mdleleni, T. Hyeon and K. S. Suslick, *J. Am. Chem. Soc.*, 1998, **120**, 6189; (*d*) H. Wang, J. J. Zhu, J. M. Zhu and H. Y. Chen, *J. Phys. Chem. B*, 2002, **106**, 3848; (*e*) J. J. Zhu, H. Wang, S. Xu and H. Y. Chen, *Langmuir*, 2002, **18**, 3306; (*f*) J. Z. Sostaric, R. A. Caruso-Hobson, P. Mulvaney and F. Grieser, *J. Chem. Soc., Faraday Trans.*, 1997, **93**, 1791.

30 A. G. Saskia, *Chem. Soc. Rev.*, 1997, **26**, 233.

31 W. Yuji, K. Hiromitsu, S. Takao, M. Hirotaro, S. Takayuki, K. Takayuki and Y. Shozo, *Chem. Lett.*, 1999, **7**, 607.

32 (*a*) D. L. Boxall, G. A. Deluga, E. A. Kenik, W. D. King and C. M. Lukehart, *Chem. Mater.*, 2001, **13**, 891; (*b*) K. W. Gallis and C. C. Landry, *Adv. Mater.*, 2001, **13**, 23; (*c*) D. L. Boxall and C. M. Lukehart, *Chem. Mater.*, 2001, **13**, 806.

33 (*a*) O. Palchik, J. J. Zhu and A. Gedanken, *J. Mater. Chem.*, 2000, **10**, 1251; (*b*) O. Palchik, R. Kerner, J. J. Zhu and A. Gedanken, *J. Solid State Chem.*, 2000, **154**, 530; (*c*) O. Palchik, S. Avivi, D. Pinkert and A. Gedanken, *Nanostruct. Mater.*, 1999, **11**, 41; (*d*) J. J. Zhu, O. Palchik, S. G. Chen and A. Gedanken, *J. Phys. Chem. B*, 2000, **104**, 7344.

34 H. Wang, J. R. Zhang and J. J. Zhu, *J. Cryst. Growth*, 2001, **233**, 829.

35 W. Tu and H. Liu, *J. Mater. Chem.*, 2000, **10**(9), 2207.

36 L. X. Yin, Y. Q. Wang, G. S. Pang, Yu. Koltypin and A. Gedanken, *J. Colloid Interface Sci.*, 2002, **246**, 78.

37 X. H. Liao, J. M. Zhu, J. J. Zhu, J. Z. Xu and H. Y. Chen, *Chem. Commun.*, 2001, 937.

38 Joint Committee on Powder Diffraction Standards (JCPDS), File No 4-0593.

39 H. Klug and L. Alexander, *X-ray Diffraction Procedures*, Wiley, New York, 1962, p. 125.

40 S. Tsunekawa, T. Fukuda and A. Kasuya, *J. Appl. Phys.*, 2000, **87**, 1319.

41 J. P. Yang, F. C. Meldrum and J. H. Fendler, *J. Phys. Chem.*, 1995, **99**, 550.

42 R. E. Mesmer and C. F. Baes, Jr., *Mater. Res. Soc. Symp. Proc.*, 1990, **180**, 85.

43 K. S. Suslick, D. A. Hammerton and R. E. Cline, *J. Am. Chem. Soc.*, 1986, **108**, 5641.